Saudi Journal of Biological Sciences 27 (2020) 2344–2357

Contents lists available at ScienceDirect

Saudi Journal of Biological Sciences

journal homepage: www.sciencedirect.com

Original article

A Chitosan-PLGA based catechin hydrate nanoparticles used in targeting of lungs and cancer treatment

Niyaz Ahmad [a,b,*], Rizwan Ahmad [c], Ridha Abdullah Alrasheed [a], Hassan Mohammed Ali Almatar [a], Abdullah Sami Al-Ramadan [a], Taysser Mohammed Buheazah [a], Hussain Salman AlHomoud [a], Hassan Ali Al-Nasif [a], Md Aftab Alam [d]

[a] Department of Pharmaceutics, College of Clinical Pharmacy, Imam Abdulrahman Bin Faisal University, Dammam, Saudi Arabia
[b] Department of Pharmaceutical Chemistry, College of Clinical Pharmacy, Imam Abdulrahman Bin Faisal University, Dammam, Saudi Arabia
[c] Department of Natural Products and Alternative Medicine, College of Clinical Pharmacy, Imam Abdulrahman Bin Faisal University, Dammam, Saudi Arabia
[d] Department of Pharmaceutics, School of Medical and Allied Sciences, Galgotias University, Gautam Budh Nagar, Greater Noida 201310, India

ARTICLE INFO

Article history:
Received 21 March 2020
Revised 2 May 2020
Accepted 11 May 2020
Available online 20 May 2020

Keywords:
Catechin hydrate
CS-CTH-PLGA-NPs
Lung cancer
Apoptosis
UHPLC-MS/MS
Lungs comparative pulmokinetics

ABSTRACT

Objective: To prepare a novel Chitosan (CS)-coated-PLGA-NPs of catechin hydrate (CTH) and to improve lungs bioavailability via direct nose to lungs-delivery for the comparative assessment of a pulmokinetics study by the first-time UHPLC-MS/MS developed method in the treatment of lungs cancer via anticancer activities on H1299 lung cancer cells.
Material and methods: PLGA-NPs was prepared by solvent evaporation (double emulsion) method followed by coated with chitosan (CS) and evaluated based on release and permeation of drug, a comparative pulmokinetics study with their anticancer activities on H1299 lung cancer cells.
Results: The particle size, PDI and ZP of the optimized CAT-PLGA-NPs and CS-CAT-PLGA-NPs were determined 124.64 ± 12.09 nm and 150.81 ± 15.91 nm, 0.163 ± 0.03 and 0.306 ± 0.03, −3.94 ± 0.19 mV and 26.01 ± 1.19 mV respectively. Furthermore, higher entrapment efficiency was observed for CS-CAT PLGA NPs. The release pattern of the CS-CAT-PLGA NPs was found to favor the release of entrapped CAT within the cancer microenvironment. CS-CAT-PLGA-NPs exposed on H1299 cancer cells upto 24.0 h was found to be higher cytotoxic as compared to CAT-solution (CAT-S). CS-CAT-PLGA-NPs showed higher apoptosis of cancer cells after their exposure as compared to CAT-S. CS-CTH-PLGA-NPs showed tremendous mucoadhesive-nature as compared to CTH-S and CS-CTH-PLGA NPs by retention time (RT) of 0.589 min, and *m/z* of 289.21/109.21 for CTH alongwith RT of 0.613 min and *m/z* of 301.21/151.21 was found out for IS (internal standard), i.e. Quercetin). Likewise, for 1–1000 ng mL^{-1} (linear range) of % accuracy (92.01–99.31%) and %CV (inter & intra-day, i.e. 2.14–3.33%) was determined. The improved C_{max} with AUC_{0-24} was observed extremely significant ($p < 0.001$) via i.n. as compared oral and i.v. in the wistar rat's lungs. The CS-approach was successfully designed and safely delivered CAT to the lungs without causing any risk.
Conclusion: CS-CTH-PLGA-NPs were showed a significant role ($p < 0.001$) for the enhancement of lungs-bioavailability and potentially promising approach to treat lung cancers. CS-CTH-PLGA-NPs did not cause

Abbreviations: CTH, Catechin hydrate; CS, chitosan; NPs, nanoparticles; CS-CTH-PLGA-NPs, chitosan-coated catechin hydrate-loaded-PLGA-nanoparticles; PVA, polyvinyl alcohol; DCM, dichloromethane; UHPLC-MS/MS, ultra high performance liquid chromatography mass spectroscopy and mass spectroscopy; ESI, Electrospray ionization; PDI, polydispersity index; SEM, scanning electron microscope; TEM, transmission electron microscope; LC, loading capacity; EE, entrapment efficiency; DSC, differential scanning calorimetry; PBS, phosphate buffered solution; CC, calibration curve; IS, internal standard; CH-S, catechin-hydrate-suspension; LLOQ, liquid–liquid extraction: LLE: lower limit of quantification; LLOQQC, lower limit of quantification for quality control; MQC, low quality control: LQC: middle quality control; HQC, high quality control; C_{max}, maximum plasma concentration; Kel, elimination rate constant; T_{max}, time to C_{max}; $t_{½}$, half-life; AUC, area under curve; LOD, lower limit of detection; LOQ, lower limit of quantitation; ANOVA, analysis of variance.

* Corresponding author at: Department of Pharmaceutics, College of Clinical Pharmacy, Imam Abdulrahman Bin Faisal University, P.O. Box 1982, Dammam 31441, Saudi Arabia.
E-mail addresses: nanhussain@iau.edu.sa, niyazpharma@gmail.com (N. Ahmad).

Peer review under responsibility of King Saud University.

Production and hosting by Elsevier

https://doi.org/10.1016/j.sjbs.2020.05.023

any toxicity, it showed safety and have no obvious toxic-effects on the rat's lungs and does not produce any mortality followed by no abnormal findings in the treated-rats.

1. Introduction

Lung cancer is biggest incidences of cancers throughout the world amongst all the type of cancers. In spite of early identification, a proper treatment, non-small-cell lung cancer is commonly diagnosed at an advanced stage through 75.0–80.0% containing already specified metastases (Brown et al., 1996; Raparia et al., 2013). The prediction of diagnosis is very poor and the survival rate for 5-year is smaller than 15% (Green et al., 2013). A new chemical entity (NCE) and their formulation is urgently required for treatment of lung cancer. It has been reported that dietary optimization is among the most effective approaches for cancer prevention (Pandey and Rizvi, 2009). Importantly, about 20% of all cases of cancer are preventable by modified diet containing high amount and variety of vegetables and fruits (Glade, 1997). Most of the natural compounds have highly contained polyphenolic phytochemicals in the fruits, vegetables, and cereal and involved in protecting plants from microbial infections, deterrence of herbivores, preventing reactive oxygen species (ROS) stress, regulation of growth processes, and ripening (Pandey and Rizvi, 2009). Polyphenol structure is characterized by the presence of multiphenol units, which might contribute to oxidative stability of plant tissue and other organoleptic characteristics, such as color, flavor, and odor (Pandey and Rizvi, 2009). Due to favorable safety profile and profound antioxidant activity, polyphenolic phytochemicals have been intensively studied as anticancer adjuvants (Lai et al., 2017; Akowuah et al., 2009; Taparia and Khanna, 2016). Particularly, in mice harboring mammary carcinoma 4T1, green tea polyphenols dramatically suppressed cancer development and inhibited tumor metastasis (Baliga et al., 2005). Green tea contained flavonoid in the form of flavanols in which mostly present catechins (Natarajan et al., 1962; Spiro and Jago, 1982). Catechins showed antioxidants property that are highly useful to the human body (Merken and Beecher, 2000; Ahmad et al., 2020a). All 6-catechins found in green tea (e.g. Catechin Hydrate) with great nutraceutical potential are water-soluble with colourless active entities which showed astringent and bitter taste to green tea infusion (Ahmad et al., 2020a; Wang and Helliwell, 2000). All catechins including Catechin Hydrate was already proved in treatment of various types of cancer like breast, colon, pancreatic, duodenum, skin, esophageal, lung, and prostate cancer (Ian and Dreosti, 1998; Kang et al., 1999; Masami et al., 1999; Mukhtar and Ahmad, 2000; Shahid et al., 2016; Jeong et al., 2017; Gujar et al., 2010; Alshatwi et al., 2015; Alshatwi, 2010; Siddiqi and Husen, 2016; Dube et al., 2010; Krishnaswamy et al., 2014).

Now a drays, various research scientists are targeting the drugs via nose–to–lungs that showed different types of useful applications like avoid hepatic first pass metabolism and non-invasive route with easy to application of drugs (Monteillier et al., 2018; Dao et al., 2018; Worth et al., 2000; Jin et al., 2019). Therefore, these PLGA-NPs. nanoparticles can be a better approach in the comparison of others. PLGANPs are known to be biodegradable, biocompatible and non-toxic and have been used for biomedical application for more than two decades. PLGA has been widely investigated for formulation of NP because of its biocompatibility, safety, ability to promote mucoadhesion and enhanced drug stability via intranasal drug delivery as compared to other routes of drug administration (Ahmad et al., 2020c; Ahmad et al., 2020d). PVA-NPs (polyvinyl alcohol-NPs) are also used similarly because of the maximum permeability, better solubility, and increase compatibility of mixtures with excellent rheological properties on the various shapes and flexibility through many types of drug delivery (Ahmad et al., 2020c, 2020d). Before designing the intranasal preparations, everyone must think the problem of little staying time of drug in the nasal cavity. This is very important for any type of optimized-formulation that should contain a highly mucoadhesive with the maximum nasal residence time. If we are going to administer any drug-formulation intranasally that it should contain a mucoadhesive property followed by enhancement of absorption of CTH-drug. Though, that dosage form should be useful to enhance the nasal retention time. Now a days, an attractive tool comes into the market i.e. nasal gel (*in situ*) formulations showed biocompatible and biodegradable-nanoparticles as a controlled release of drug like CTH (Ahmad et al., 2016a; Fernandez-Urrusuno et al., 1999; Md et al., 2013; Ahmad, 2017; Ahmad et al., 2020d). A great attention have been developed now a days about the polymeric-NPs that showed longer therapeutic action, control rate of drug release with maximum drug-loading (DL), increasing their surface area. Thus, the release of drug will fast initially followed by maintaining the drug therapeutic level as compare with other carriers and drug-delivery for the targeted to particular sites of the body. These polymeric nanoparticles provide the some other additional useful applications as compared to other drugs-formulations delivered through nose–to–lungs because these- nanoparticles protect the drugs via encapsulation stay away from the direct participation of biological degradation to increase the bioavailability of drugs into the lungs.

Likewise, literature survey (Jaitz et al., 2010; Sapozhnikova et al., 2014; Svoboda et al., 2015; Taamalli et al., 2015; Dias et al., 2013; Poon et al., 1998; Chang et al., 2011; Nelson et al., 2003) reports different methods for green tea or tea or coffee extracts, fruits juices, and other plants extracts for analysis of samples. However, they published concurrent development with various catechins at the similar time, i.e. plasma analysis is any reports not available for Catechin Hydrate alone. There are two methods developed for catechins for the analysis of brain and urine samples (Lendoiro et al., 2014; Ahmad et al., 2020a). Besides this, it is very important for current study is lack of availability of any method for lungs as well as plasma bioanalysis of single-CTH-only with very lesser time upto picogram level. In the current study, a novel bioanalytical UPHPL-MS method was successfully developed, validated, and applied for all pulmokinetics parameters evaluations of CS–coated–PLGA–NPs by UHPLC-ESI-triple-quadrupole-MS/MS. The current study showed a bioanalytical method contained various applications in terms of higher sensitivity, highest efficiency, and very low retention with very less total run time for the estimation of pulmokinetics parameters in lungs as well as plasma.

This is a first time development of novel chitosan (CS)–coated–PLGA–NPs to increased lungs targeting of CTH. The major objective is to improve the bioavailability of CTH in the lungs after the i.n. delivery of optimized-CS-CTH-PLGA-NPs to achieve an improved CTH-therapeutic level in the lungs. It was also avoided the unrequested systemic exposure of CTH alongwith required optimum dose for therapeutic-level of lungs. CS-CTH-PLGA–NPs were showed excellent effective-solubility and their permeability. Optimized-CS-CTH-PLGA-NPs were characterized by many physic-

ochemical parameters to estimate their suitable CTH-delivery of nose-to-lungs. A comparative pulmokinetics study was performed via delivery of CS-CTH-PLGA-NPs from different routes (i.v., oral, and i.n.) in wistar rats. The quantification of CAT in lungs was carried out via a newly developed bioanalytical UHPLC-MS/MS method in the lungs for the treatment of lungs cancer by cancer cell lines. Further evaluation of the formulated NPs was performed on human non-small cell lung carcinoma (NSCLC) H1299-cell-lines to evaluate cytotoxicity, apoptotic potential and to evaluate the cell cycle arrest potential. Finally, the toxicity study was successfully established which is an important parameter for the safety of newly developed-NPs.

2. Materials and methodology

We have bought 99.98% purity CTH from AK Scientific, Inc. 30,023 Ahern Avenue Union City, CA 94587, USA. CS, PVA (MW 25000), and PLGA from Tokyo Chemical Industry Co., Ltd. 6-15-9 Toshima, Kita-ku, Tokyo 114-0003 and Polysciences Inc, 400 Valley Road were bought. DCM was bought from Sigma Aldrich Corporation (St. Louis, MO, USA). All the analytical solvents were bought from Sigma-Aldrich. The whole analysis was performed with the help of Milli Q Water. The apoptosis detection kit was bought from BD Bioscience.

2.1. Development of NPs

For the preparation of PLGA NPs, we slightly modified Ahmad et al method based on double emulsification (w/o/w) solvent evaporation method (Ahmad, 2017; Ahmad et al., 2020a). CTH was solubilized in PVA solution (1.10%w/v) to prepare an aqueous as a internal phase (IAP). PLGA was solubilized in DCM to form organic phase. Probe sonicator (Ultrasonic processor, Sonopuls, Bandelin, Germany) was used to emulsified IAP in the organic phase for 4.0 min at voltage efficiency (60.0%) wit temperature (25.0 ± 1.0 °C) to prepare w/o as a primary emulsion (PE). PE has been additionally emulsified through sonication by various PVA concentration solution or EAP (external aqueous phase) to obtain a 2°-emulsion (w/o/w). For the evaporation of organic solvent, 2°-emulsion was kept on magnetic stirrer upto 4 to 5 h. NPs were found in the form of suspension, it was centrifuged at 15000.0 rpm (30.0 min) followed by rising for three-times for the removal of extra amount of PVA as well as CTH sticked on the NPs-surface. Opt-NPs were washed pellets and dispersed in the 5.0%w/v mannitol solution followed by dried with help of freeze dryer (Lab Conco., LPYH, Lock 6, USA freeze dryer) at −60.0 °C (upto 24.0 h) to get freeze-dried-NPs.

A specific amount of CTH-PLGA-NPs suspensions is incubated CS-volume (2.0 mg/ml) in 0.50% acetic solution for 2.0 h at room temperature (Ahmad, 2017; Ahmad et al., 2020a). Obtained-CS-CTH-PLGA-NPs were centrifuged followed by two times washing and after that redispersed in the Milli-Q-water (predetermined volume). Resulted-NPs were dispersed and stabilized with the help of Lyophilizer (Lab Conco., LPYH, Lock 6, USA freeze dryer) for 3.0 days (at −60.0 °C). Resulted CS-CTH-PLGA-NPs were formulated in triplicate.

2.2. Characterizations of CS/CTH-PLGA-NPs

2.2.1. PDI, ZP, and particle size

Particle size determination is the very essential parameter. If particle size decreases parallely increases the surface area for the absorption of drug (Ahmad, 2017; Ahmad et al., 2020a). PDI, particle size, and ZP for the opt-nanoformulation were examined through Dynamic light scattering technique (Malvern–Zetasizer, Nano–Zetasizer, UK). Dilution is very important to before analyze the particle size. At the time of particle size analysis, we have maintained the temperature 25.0 °C and 90° fixed the scattering angle (Ahmad, 2017; Ahmad et al., 2020a). The samples were diluted to used and analyse size and surface charge of nanoformulations, where each measurements were prepared in triplicate. At the time of particle size analysis and their surface charge for NPs, we determined the samples in triplicate.

2.2.2. SEM (Scanning electron microscopy)

We adopted to use Ahmad et al method to examine the shape of particles via SEM (FEI, INSPECT S50, Czech Republic) (Ahmad, 2017; Ahmad et al., 2020a).

2.2.3. TEM (transmission electron microscopy)

We adopted to use Ahmad et al method to examine the size of particles via TEM (FEI, MORGAGNE.68, Czech Republic) (Ahmad, 2017; Ahmad et al., 2020a).

2.2.4. EE (%Entrapment Efficiency), LC (%Loading Capacity), and Process Yield (%)

LC and EE of NPs were estimated through the ultracentrifugation for 30.0 min at 15,000 rpm at 4.0 °C. Our in house-developed UHPLC–MS/MS method helped to determine the CTH-free amount from supernatant (Ahmad, 2017; Ahmad et al., 2020a). EE and LC calculated on the basis of mentioned below equation for opt-NPs (Ahmad, 2017; Ahmad et al., 2020a):

$$\mathrm{EE}(\%) = \frac{\text{Whole CTH Quantity} - \text{Free CTH Amount}}{\text{Whole CTH Quantity}} \times 100$$

$$\mathrm{LC}(\%) = \frac{\text{Whole CTH Quantity} - \text{CTH Free Amount}}{\text{NPs Weight}} \times 100$$

Process Yield (%) was calculated through mentioned below formula:

$$\text{Process Yield } (\%) = \frac{W_1(\text{Dried NPs Weight})}{W_2(\text{overall weight of dried initial material})} \times 100$$

2.3. Differential Scanning calorimetry (DSC) study

CTH (Pure Catechin), PLGA, PVA (Poly Vinyl Alcohol), CTH, PLGA, PVA-physical mixture, lyophilized CTH-PLGA-NPs, Pure CS, and CS-CTH-PLGA-NPs samples were analysed by DSC 214 Polyma (NETZSCH Wittelsbacherstraße 42, 95,100 Selb, Germany). 10.0 mg of every sample was taken inside pan which was made up of aluminium and then crimped after that 20.0–400.0 °C heated with 10.0 °K/min rate with N_2 gas continuously-supplied (Ahmad, 2017; Ahmad et al., 2020a).

2.4. In vitro drug release

The *in vitro* release of CTH from the CTH-PLGA-NPs & CS-PLGA-NPs were carried out in two separate release-medium with pH 7.40 and pH 5.50 in order to initiate the physiologic and acidic condition of cancer cells with slight modification (Ahmad et al., 2018a; Ahmad et al., 2019; Ahmad et al., 2020b). Equal quantities of CTH-PLGA NP samples were packed in a dialysis sac and suspended in a 25.0 ml of the respective release medium having different pH 5.50 and pH 7.40. A similar set of release study of the CS coated CTH-PLGA NP samples were continued. In both the cases, temperature was maintained at 37 °C in a paddle type dissolution apparatus where the speed of paddle was set to 100 rpm. At a particular interval of time, 1.0 ml sample aliquots were collected and

replaced with equal volume of fresh buffer. 1.0 ml every test sample was withdrawn from each sampling-time point. After the withdrawal of every test sample, it was filtered through 0.20 μm syringe-filter and then analysed by UHPLC–MS/MS-method (Ahmad et al., 2018a; Ahmad et al., 2019; Ahmad et al., 2020b).

2.5. Ex-vivo study based on nasal mucosa based permeation

Local slaughterhouse has provided the fresh nasal tissues from the goat's nasal cavities. A fix area i.e. 0.785 cm^2 for tissue cells was taken for the permeation of CTH (Logan Instrument Corporation, Piscataway, NJ). A saline 20.0 ml phosphate buffer (pH: 7.40, at 37.0 °C) was taken into the receptor chamber as in a each and every separate pure-CTH-suspension, lyophilized-CTH-PLGA-NPs and lyophilized-CS-CTH-PLGA-NPs (∼CTH: 10.0 mg) were taken in the donor chamber (21.50–2.0 ml) after pre-incubation-time for 20.0 min in each analysis. 500.0 μl samples were withdrawn from receptor chamber based on predetermined time intervals. All the samples filtered through 0.20 μm syringe-filter and then analysed by UHPLC-MS/MS-method (Ahmad et al., 2016b).

2.6. Cytotoxicity of free CAT and CS-CAT-PLGA NPs

Prediction of cytotoxicity of investigational agents in different cells is among the first *in vitro* bioassay techniques, which usually provides the basis of crucial means of screening and safety assessment of the investigational agent (Tolosa et al., 2015). Therefore, the MTT colorimetric assay was conducted in NSCLC cell line (H1299) with free CAT, CS-CAT-PLGA NPs and placebo CS-PLGA NPs. The specific number of H1299 cells (6×10^3 cells) were seeded in each well of the 96-well plate for a period of 24 h. The incubated cells were then treated with various concentrations (5–100.0 μg ml^{-1}) of free CAT, CS-CAT-PLGA-NPs and placebo CS-PLGA-NPs. Following an incubation period of 24.0 h the treated samples were removed from the wells and the cells were incubated with 25.0 μl of MTT solution (0.50%, w/v) for 4.0 h at 37.0 °C. Later after incubation, the unreacted MTT solution was removed and the cells were exposed to 150 μl DMSO in each well for a period of 20.0 min to solubilise the formed formazan crystals. At last, the absorbance of the formazan solution in each well was examined at 570.0 nm via microplate reader (Thermo Fisher Scientific, Waltham, MA), which was proportionate with the number of viable cells in the wells. Viability of the treated cells was calculated comparing with control cells and reported.

2.7. Induction of apoptosis in H1299 cells by free CAT and CS-CAT-PLGA-NPs

The technique (Double staining) was used to analyse apoptotic potential of the free CAT and formulated NPs. In due course, the H1299 cells were seeded in 6-well plates where the cells are incubated with free CAT and CS-CAT-PLGA-NPs. Following an incubation of 24.0 h, cells washing were performed two times with cold phosphate buffer saline. The cells are then re-suspended in binding buffer and treated with 5.0 μl of Annexin V–fluorescein isothiocyanate (FITC) conjugate and 5.0 μl propidium-iodide. The cells were stained following an incubation of 15.0-min in dark at room temperature. The cells were then analysed through flow cytometry (BD FACS AriaTm III) and obtained data were evaluated via FACS DIVA 8.0.2.

2.8. Western blotting

CAT and CS-CAT-PLGA-NPs effect was evaluated by the Bax and Bcl-2 apoptotic expression markers with the help of analysis of western blot in the lung cancer (H1299) cells. CAT and CS-CAT-PLGA-NPs incubated with H1299 cells were seeded in six-well plates. PBS was used to wash all the cells and radio-immunoprecipitation assay lysis buffer (RIPA buffer) was used for incubation for thirty minutes on the ice. The supernatant liquid samples were collected after 12,000.0 rpm centrifugation at 4.0 °C that contained the proteins. SDS-PAGE was used to separate out the all extracted proteins and then it transferred to PVDF membranes. 5.0% BSA and TBST were used to keep the membrane for 2.0 hrs at room temperature to obstruct every binding site on the membrane. Primary antibodies to β-actin, BAX and Bcl-2 were use to incubate the membrane. The membrane was incubated after 10.0 h with horseradish peroxidase-conjugated secondary antibodies for 1.0 h. Chemiluminescence reagent kit was used to identify the signal and imagined protein bands quantification was carried out through densitometric analysis with the help of image J software.

2.9. CAT and CS-CAT-PLGA-NPs induced cell cycle analysis

H1299 cells were used to verify the effect of free CAT and formulated NPs on the cell cycle distribution (Min et al., 2018). The cells were incubated in 96-well plate with a fixed concentration of CAT in different formulation. Then the cells were harvested and were fixed with 75% ethanol at 4.0 °C for 30 min. The cells were washed again with phosphate buffer saline twice and re-suspended in 50 mg/mL propidium iodide solution containing 50 ng/mL of RNase for 30 min in the dark at room temperature. The number of cells was tested subsequently with the help of flow cytometer (BD FACS AriaTm III). Ten thousands cells data were collected from every data file in which were acquired data were analysed with the help of FACS DIVA 8.0.2 software.

2.10. Animal study

For the pulmokinetics study, we have taken the ethical approval from Imam Abdulrahman Bin Faisal University Ethical Committee (ethical approval number IRB-UGS-2019–05). Each cage has 4–5-rats (weight; 200–250 g). We have maintained natural light with dark cycle followed by the easy way to reachable food & water and also maintained the temperature 20–30 °C with 50–55% humidity.

2.11. UHPLC-MS/MS bioanalytical method development and their validation (MDMV)

US–FDA, 2001 guidelines were followed for MDMV for CTH. Eight different standard points were selected to plot CC (calibration curve) for linearity with the calculation of peak area ratio; $1/x^2$ regression was employed. Signal to noise was used 10:1 to measure lower limit of quantification (LLOQ) and LOD (Lower limit of Detection). We have withdrawn 6-pre-spiked of extracted samples to analyse by mean area response vs. post-extraction spiked CTH-free in the matrix (lungs and plasma). Same way, we determined recovery of IS samples. We analysed inter and intra-day accuracy and precision through the selection of LLOQQC, LQC, MQC, and HQC (for each QCs: 6-replicates) with one CC of lungs homogenate and plasma samples.

2.12. Required conditions for UHPLC-MS/MS

UHPLC–MS/MS exhibited a binary solvent manager with autosampler was used that contain high resolution and very sensitive tunable mass detector (LCMS-8050, ESI, Triple Quadrupole, Japan). Pinnacle DB C18 (1.9 μm; 50.0 × 30.0 mm) column was used with a mobile phase (Acetonitrile: Water::91:09), 2.0 μl injection volume, with a flow rate (0.400 ml min^{-1}) and total run time

was 1.5 min. LCMS-8050 was used to determine the mass of the samples with the application of collision gas (Argon gas), scan time (1.0 min), inter-scan delay (0.020 sec with 0.10 μ scan step: 30,000.0 micro sec^{-1}). Collision energy (25.0 eV CE for CTH and 21.5 eV for Quercetin) were selected for the quantification of CTH & IS in the negative ion mode. The *m/z* 289.21/109.21 and 301.21/151.21 transitions were used to bioanalysis of samples for CTH and Quercetin (IS), respectively. Lab Solution Software (V5.93) was used to calculate the exact mass determination with the amount of analyte as well as assessment of parent and daughter ions.

2.13. CC and QC samples preparation

CTH stock solution was prepared first in the methanol (10.0 mg 10.0 $ml^{-1)}$. The various 8-CC concentrations were prepared like analyte (2.0% aqueous) in the blank matrix (plasma or lungs homogenate) of the rats that means matrix (980.0 ml blank) + analyte (20.0 ml of aqueous). CC-range (1.0–1000.0 ng ml^{-1}) for CTH was prepared in different sampling matrixes points like 1, 2, 22, 208, 420, 638, 850, and 1000 ng ml^{-1}. In a same way, all the QCs HQC (805.00), MQC (420.00), LQC (2.91), LLOQC (1.010), and IS (50 ng ml^{-1}) were prepared water: methanol (1:1) mixture. The temperature (2–8 °C) stored all spiked freshly diluted.

2.14. Different types of matrix samples extraction

Lungs homogenate or plasma unknown samples with fresh known samples (CC and QC) were prepared and collected for bioanalysis. Each aliquot (550.0 μl) has taken in a fresh cleaned glass tube after that added IS (50.0 ng mL^{-1}; 100.0 μl). After that, formic acid (200.0 μl; 5%) was added with vortexed (300 rpm) for 5–6 min to break the matrix protein. The samples was centrifuged at 4000 rpm (for 10 min at 4 °C) followed by transferred supernatant sample (4 ml) in a clean glass tube. All these samples were evaporated on water-bath (37 ± 1 °C) with the help of samples dried under nitrogen stream. We have reconstituted residues by mobile phase (700.0 μl) in order to vortexed (300 rpm) for 5 min. UHPLC vials were used to transfer the reconstituted residues for bioanalysis.

2.15. Pulmonokinetics

In this study, optimized-CS-CAT-PLGA-NPs have used for their comparative pharmacokinetics study via delivery of CS-CAT-PLGA-NPs from different routes (i.v., oral, and intranasal) in wistar rats. On the basis of results, we are able to know the best route for lungs targeting drug delivery. For pulmonokinetics and actual reached CAT of CS-CAT-PLGA-NPs, rats were divided into three groups (6x3 = 18). The study was carried out at seven preselected time points of 0.25, 0.50, 1, 2, 4, 8, 12 and 24 hrs. Eighty one wistar rats in three groups (27 × 3 = 81) were randomly distributed as; Group-I: i.v., Group-II: oral, Group-III: intranasal. For bioanalytical determination of CAT in lungs and plasma, three animals at each time point were sacrificed to obtain plasma and lung homogenate.

2.16. In vivo Histopathological examination of CS-CAT-PLGA-NPs toxicity

Wistar rats were selected for CS-CAT-PLGA-NPs toxicity evaluation as this animal model offered a large surface area for intranasal to lungs of CS-CAT-PLGA-NPs and to accurately determine the CS-CAT-PLGA-NPs toxicity on the lungs as per the method reported by Bao et al. (2015) and Menon et al. (2017). All rats were sacrificed and then removed the lungs intact extraction after 7-days treatment. It was inflated through 4.0% paraformaldehyde tracheal instillation at 25.0 cm water airway pressure. The paraffin was used to embed the tissues and then sectioned. All the tissues stained with hematoxylin and eosin stain.

2.17. Evaluation based statistics

All the data was analysed like mean ± SD (standard deviation). For data comparison ANOVA with $p < 0.05$ was applied as a statistical tool. The software used for analysis was GraphPad v 3.0 (San Diego, CA).

3. Result and discussion

3.1. Nanoformulation development and their characterizations

PLGA NPs were prepared using PLGA and PVA through double emulsification-solvent evaporation method, where PVA acts as stabilizer of the formulation. Here, the particles size was reduced by ultrasonication techniques at nano-range followed by lower PDI. PLGA-NPs showed the particle size range 119.34 ± 11.61 nm in which DL didn't exhibited any significant enhance the NPs sizes. A significant enhance in particles size were determined 150.81 ± 15.91 nm while the PLGA-NPs were coated with CS (Table 1). Incorporation of CAT within the nanostructure has shown to increase the PDI of the formulation significantly, however, in all the cases of the formulated particles were identified with <0.310 PDI, representing monodisperse nature of the particles. As depicted in Fig. 1 and Table 1, the surface charge of the opt-PLGA NPs were determined almost constant, slightly negative or near to the neutral (e.g., −4.10 ± 0.20 mV for CAT-PLGA-NPs). Comparatively after the nanoparticles coating, it was observed a significant change on the surface of NPs i.e. positive 26.01 ± 1.19 mV (for CS-CTH-PLGA NPs). It was also enhanced the stability of the NPs (Fig. 1B). CS have amino groups that is helpful to the enhanced the +ve ZP, it recommended that the CTH-PLGA NPs were satisfactorily coated through CS. CS-CTH-PLGA NPs contained +ve charge on their surface that enhances the adhesion and retention via cancer cells that are –vely charged membranes (Fig. 2) (Wang et al., 2013). CS coated NPs decreases chances of NPs interactions with phagocytes and their absorption via these cells for the reason that +vely charged NPs are a very smaller absorption (Parveen and Sahoo, 2011). TEM and SEM microimages showed the smooth surface and spherical CS-CTH-PLGA NPs (Fig. 3). EE of CAT within the PLGA nanocarrier was calculated as percentage ratio using the equation provided in the methodol-

Table 1
Average particle size, polydispersity index (PDI) zeta potential, %entrapment efficiency, %drug loading, %Yield of optimized formulations.

Formulations Type	Average PS (nm) ± SD	Average PDI ± SD	Average ZP (mV) ± SD	Average Yield (%) ± SD	Average EE (%) ± SD	Average DL (%) ± SD
PLGA NPs	119.34 ± 11.61	0.116 ± 0.05	−3.94 ± 0.19	–	–	–
CTH-PLGA NPs	124.64 ± 12.09	0.163 ± 0.03	−4.10 ± 0.20	91.65 ± 4.01	72.34 ± 2.68	5.53 ± 0.16
CS-PLGA NPs	146.69 ± 15.68	0.291 ± 0.02	27.51 ± 1.31	–	–	–
CS-CTH-PLGA NPs	150.81 ± 15.91	0.306 ± 0.03	26.01 ± 1.19	95.48 ± 4.57	76.48 ± 4.51	8.76 ± 1.31

Results expressed as mean ± SD (n = 3). SD: standard deviation; NA: not applicable; NPs: nanoparticles. CTH: Catechin Hydrate, CS: chitosan.

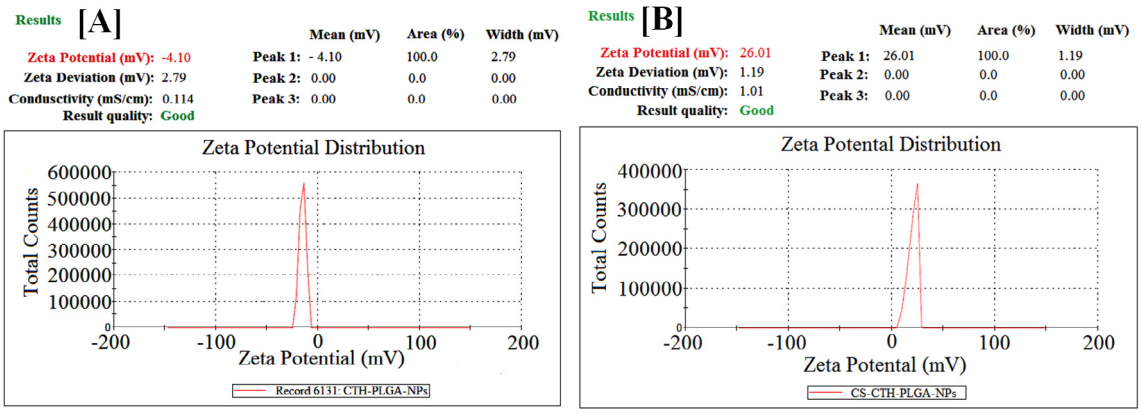

Fig. 1. Zeta potential of PLGA NPs suspended in PBS (pH = 7.4), **[A]:** CTH-PLGA-NPs; **[B]:** CS-coated-CTH-PLGA-NPs.

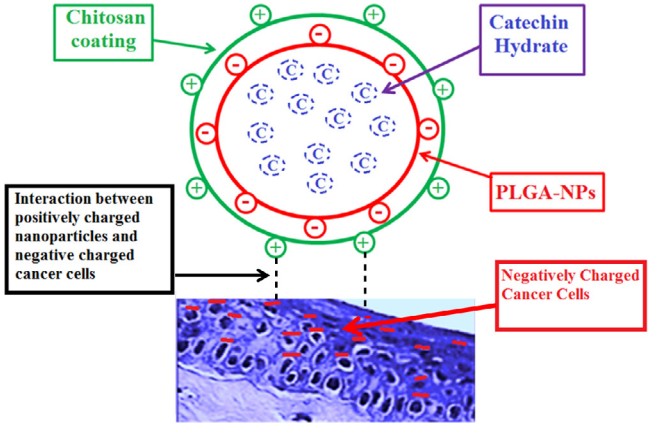

Fig. 2. Schematic presentation of chitosan-coated PLGA NPs and their interaction with cancer cells. The positive surface of nanoparticles promotes adhesion and retention by cancer cells, which have negatively charged membranes.

ogy section. With the change in concentration of PLGA, the %EE of CAT was varied proportionately within the PLGA-NPs, however, optimized formulation of CS coated CAT-PLGA-NPs were found to encapsulate 76.48 ± 4.51% with 8.76 ± 1.31 %DL. CS was coated on opt-CAT-PLGA-NPs that enhances the mucoadhesive and retention time in the nasal region. After that; we have our main objective i.e. opt-CS-CAT-PLGA-NPs were examined by *in-vitro* CTH-release, *ex vivo* permeation, H1299 cells cell lines, and their pulmokinetics study. Based on our findings, opt-CS-CAT-PLGA-NPs have been fruitfully coated on CTH-PLGA-NPs for the delivery of CAT via intranasal route. At last our conclusion is CTH adsorbed on the surface of opt-NPs due to CS (+vely charged) and CTH (−vely charged –OH hydroxyl ion) electrostatic interaction (Ahmad, 2017; Ahmad et al., 2018a). 26.01 ± 1.19 mV ZP showed the stability of opt-CS-CTH-PLGA NPs (Fig. 1B). Positive-charge on the surface of opt-CS-CTH-PLGA NPs facilitates to enhanced mucoadhesion with increment of residence time and decreases the mucociliary clearance of opt-CS-CTH-PLGA NPs from the nasal mucosa (Md et al., 2013; Ahmad, 2017).

PLGA polymer was used to prepare our CAT based nanoformulation in which for the stabilization, PVA was integrated. Generally for the formulation of PLGA-NPs, stabilizer was used i.e. PVA that is easily binds to PLGA with the help of PLGA interpenetration and PVA molecules at the time of preparation of nanoparticles (Ahmad, 2017; Ahmad et al., 2020a). PVA was used as a copolymer that exhibited polyvinyl alcohol & polyvinyl acetate by distinctive block copolymer in which vinyl part represents lipophilic property. PVA (lipophilic segment) is recognized and used as a penetrating agent for organic phase at the time preparation of NPs whereas from polymeric matrix used as elimination of organic solvent and it was finally resulted that PVA was entrapped inside the PLGA-matrix (Sahoo et al., 2002). The decrement of particle size was due to the use of ultrasonication technique in the dispersed phase where these NPs as a nanocarrier showed a uniform characteristics nature in the size-range of 119.34 ± 11.61 nm. Ahmad et al reported before content selection of polymer, copolymer, and

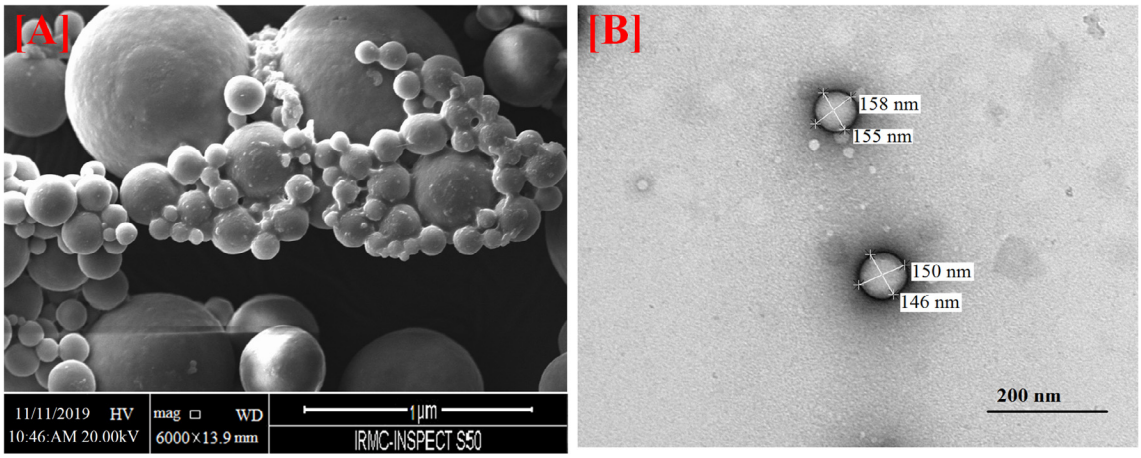

Fig. 3. Scanning electron microscopy (SEM) **[A]** and transmission electron microscopy (TEM) **[B]** images of CS-coated-CH-loaded-PLGA-NPs.

selected-drug at the time of preparation of NPs and the loading of drug inside the PLGA NPs followed by a required nanoparticles size range (Ahmad, 2017; Ahmad et al., 2020a). A smallest PDI was observed for our opt-CS-CTH-PLGA NPs which showed very small differences in all the batches at the time of nanoformulation development. Although loading of drug within the NP formulation showed to increase the PDI significantly, the value did not exceed 0.306, indicating formation of unimodal particles (Budhian et al., 2008). CS-coating on the PLGA-NPs represented a significant ($p < 0.05$) enhance in particles size. On the other hand this change in particle-size did not affect the mean PDI as compared with uncoated particles. Finally, it was designated no agglomeration of the particles after coating with the CS.

3.2. Differential scanning calorimetry (DSC)

CTH, PLGA, PVA, CTH + PVA + PLGA physical mixture, opt-CTH-PLGA NPs dried from lyophilizer, CS pure and opt-CS-CTH-PLGA NPs of DSC thermograms were displayed in Fig. 4. There are two major peaks i.e. one in-between 90 and 110 °C related to loss of water and other peak at 170.3 °C which is related to anhydrous CTH and also it showed mp i.e. very closed to reported mp 175 °C. Finally, it was decomposed >200 °C. In the same way, CTH + PVA + PLGA physical mixture showed all the characteristic peaks. There was no peak in CTH-PLGA-NPs. It represents CTH entirely entrapped inside CTH-PLGA-NPs. A very distinctive peak was observed in-between 45.0 and 55.0 °C in PLGA pure polymer and also opt-PLGA NPs (Fig. 4) (Ahmad, 2017; Ahmad et al., 2018a). One exothermic broad peak was shown at 310.7 °C for CS but other peaks were endothermic i.e. 160.2 °C & 193.8 °C. It was shown again in opt-CS-CTH-PLGA NPs at 310.8 °C. In Fig. 4, CS-CTH-PLGA NPs showed again CS peak due to CS coated on CAT-PLGA-NPs. One more a very small peak of PLGA has been distinguished at 52.6 °C that could be lesser % of chitosan quantity compare to % of PLGA other side CTH-peak was not observed in the opt-CS-CTH-PLGA (Fig. 4) (Ahmad, 2017; Ahmad et al., 2018a).

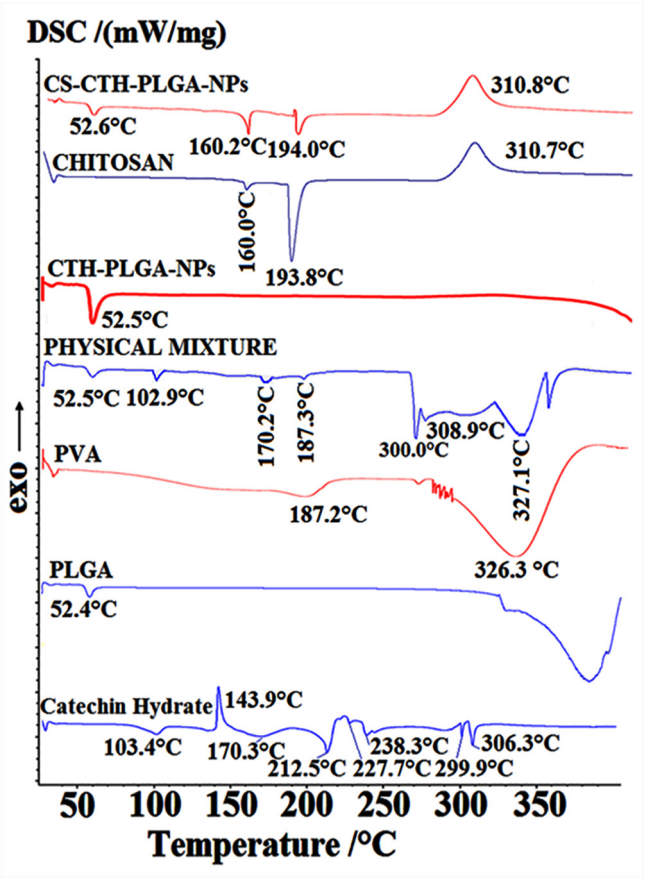

Fig. 4. The DSC thermograms of Pure–Catechin (CTH), Polymer (PLGA), Poly Vinyl Alcohol (PVA), Physical Mixture of CTH, PVA, with PLGA, freeze–dried–CTH–loaded–optimized Polymeric (PLGA)–NPs, Pure Chitosan, and CS-Coated- CTH–loaded–optimized Polymeric PLGA–NPs.

3.3. In vitro CTH release evaluation

Any drug release from NPs delivery is very important to create intended physiological response that should be successfully changed via modification of physicochemical medium characteristics. CS coated CAT-PLGA is applied to transport the entrapped CAT within the cancer microenvironment, nanoformulations release study was evaluated at 2-different pH: 5.50 and 7.40, which roughly corresponds to the pH of the tumor microenvironment, different cellular compartments, and also for nasal mucosa respectively. CAT-release profiles from the NPs at various pH values were displayed in Fig. 5A, where it is clearly be demonstrated that the release of CAT from the PLGA NPs and CS-PLGA NPs were 67.01% and 80.93 ± 5.64% respectively at pH 7.4. The PLGA NPs showed burst release of 26.01% at 2.0 h whereas CS coated PLGA NPs showed 41.06 ± 2.98% drug releases. This result demonstrate that initial release of CAT in CS coated PLGA NPs was significantly greater than that in PLGA NPs and showed more sustain release at pH 7.4. At pH 5.5 the release rate of CAT in CS-coated PLGA NPs was very fast and CAT was released at 2.0 h whereas only 23.14 ± 1.51% drug release for PLGA NPs. This result indicating that CS coated PLGA NPs had pH-responsive properties. The release CAT from the PLGA-NPs was found to be sustained over a period of 24.0 h, with a cumulative release of 78.02 ± 4.41% at pH 5.5 in Fig. 5B.

It is important to bring into discussion that the surface charge and size of the nanocarriers are believed as most important determinants for improved permeability and retention (EPR) effect, where the size of the particle facilitate prolong retention within the systemic circulation escaping the reticuloendothelial cells, whereas charge of the particle facilitate to target to particular site and release the drug (Choudhury et al., 2019). Therefore, the nanometric size of the current nanoformulations will facilitate prolong systemic circulation; thereby assist in passive targeting of the entrapped drug to the porous tumor area (Gorain et al., 2018). Further, it has also been revealed that the surface of the tumor cells are translocated with a negatively charged residue, phosphatidyl choline (Pandey et al., 2018), which facilitate binding of positively charged particles. The charge of the CAT-PLGA NPs was slightly negative in nature due to the presence of ionized carboxylic groups. Amphiphilic PVA presence forms a stable fence on the polymer surface, however, this fence of PVA shield the surface charge of the NPs and transfers the shear plane outer to the particle surface. Consequence of which, the surface charge of the NPs were recorded in slight negative zeta potential (Sahoo et al., 2002). On the other hand, CS, the weak base polysaccharide, consists of β (1,4) linked monomers of N-acetyl-D-glucosamine and D-glucosamine, in which the surface amino groups are ionized in acidic environment to provide positive charge (Nafee et al., 2007). Therefore, the presence of positively charged amino groups on CS alters the ultimate surface charge of the CS coated NPs to positive. This shifting in surface charge upon CS coating on the PLGA NPs is clearly reflected in Fig. 1. Thus, positive charges of the CS-coated CAT-PLGA NPs is thought to potentiate binding of the nanocarriers to the surface of the negatively charged tumor cells during prolong circulation of the NPs within the circulation due to EPR effect.

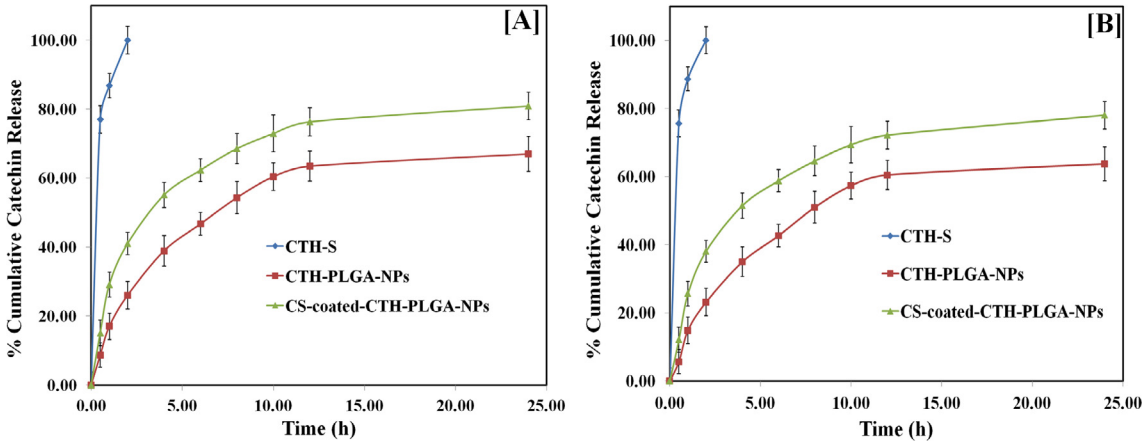

Fig. 5. **[A]** *In vitro* release profile of CTH-S, CTH–loaded–PLGA–NPs and Chitosan-coated-CTH–loaded–PLGA–NPs performed by using dialysis bag method, revealing sustained release pattern of CTH–loaded–PLGA–NPs and Chitosan-coated- CTH–loaded–PLGA–NPs (Temp was set at 37 °C, mean ± SD, n = 3) at pH 7.4 **[A]** and at pH 5.5 **[B]**.

Further, modulation of release of the entrapped drug in any carrier is utmost important to avoid unfavorable side effects due to exposure of the normal cells to the released drug. Therefore, current formulation approach is planned to modulate the release of entrapped drug (CAT) within the cancer microenvironment. To accomplish this goal, we have coated the CAT-PLGA NPs with CS, which will primarily release the drug at a particular pH of the cancerous environment. It is relevant to mention that the pH of the cancer microenvironment is acidic and ranges from 5.5 to 7.0, due to hypoxic condition during uncontrolled proliferation, deficient blood perfusion and glycolytic cancer cell metabolism (Justus et al., 2013). Therefore, to ensure the release of the entrapped drug within the acidic environment and decreased systemic exposure of the drug, we have evaluated the release study in two different pH, 5.5 and 7.4, which roughly corresponds to the cancer environment and systemic circulation. The demonstrated result reflects release of the formulation from the CS coated CAT-PLGA NPs rapidly within the acidic environment, whereas the release pattern in physiological pH was slow. Thus, we can assume that the developed NPs formulation would stay in the circulation without releasing the entrapped drug, whereas, if the formulation reaches to the site of action, will release the entrapped drug rapidly to exert its physiological role.

3.4. Ex vivo nasal mucosa permeation study

The permeation showed significantly maximum for CS-CTH-PLGA NPs ($p < 0.001$) > CTH PLGA NPs ($p < 0.01$) > CTH-S (Pure) (Fig. 6A). Maximum permeation was shown by CS-CTH-PLGA NPs i.e. >82.93 ± 5.91% while 67.98 ± 4.71% for CTH-PLGA-NPs and 20.65 ± 3.01% for CTH-S only (Fig. 6A). CS has positive charge due to amino group on C2 position that is responsible for interaction to negatively charged membranes of cells therefore, CTH showed enhanced the permeation. Same way, epithelial mucosal cells were also participated to support the mechanism of their tight junctions (Md et al., 2013). The permeation of pure CTH was very little that represents hydrophilic nature of CTH for excellent justification. Maximum permeability showed with hydrophobic drugs by nasal mucosa or skin reported by Richter and Keipert, 2004. CS-CTH-PLGA-NPs has their surface i.e. lipophilic with <165.0 nm size NPs easily permeated to biological membrane. At last it is concluded based on above observations: NPs contain lowest size, higher yield (%), maximum % EE with maximum % DL is mainly accountable for maximum permeation of CS-CTH-PLGA-NPs that will offer superior outcome for *in vivo* activity.

3.5. Cytotoxicity of CAT and CS-CTH-PLGA NPs

Keeping in view the importance of cytotoxic agents and corresponding cell death assays in cancer drug discovery (Bahuguna et al., 2017), we evaluated the cytotoxic potential of CAT and its nanoformulations (CS-CTH-PLGA-NPs) on NSCLC cell line H1299. The cytotoxicity was examined by MTT [3-(4, 5-dimethylthiazolyl-2)-2,5-diphenyltetrazolium bromide] assay. The prepared formulations were tested on the human non-small cell lung cancer cell line H1299 was applied to identify the effects

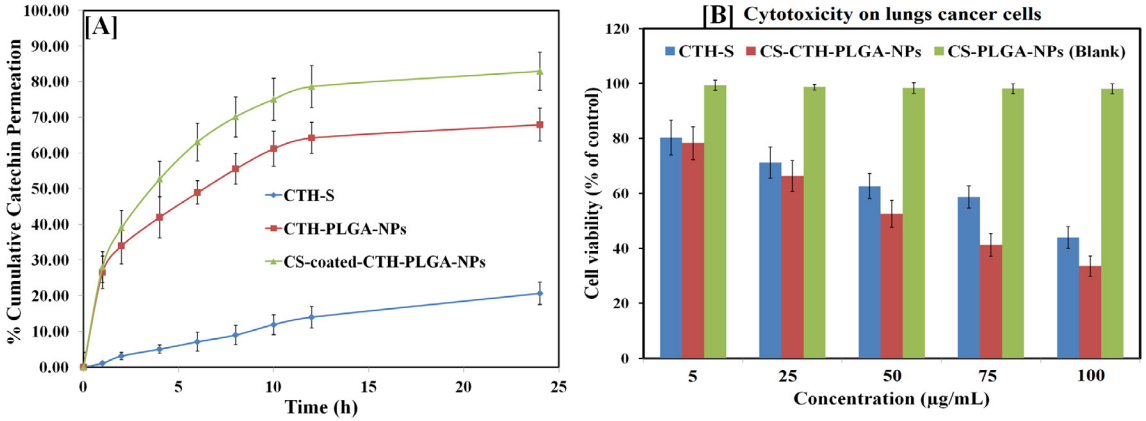

Fig. 6. **[A]** *Ex vivo* permeation profiles of developed Chitosan-coated-CH–loaded–PLGA–NPs as compared to CTH–loaded–PLGA–NPs and pure CTH-S through goat nasal mucosa. **[B]** Cell viability of H1299 cancer cells after 24 h exposure of (A) CTH solution, CS-CTH-PLGA-NPs, and CS-coated PLGA NPs (blank/placebo) nanoformulations. The cell viability was determined by MTT assay. Control consisted of cells treated with 0.1% DMSO (vehicle control, 100% cell viable). Data are expressed as mean ± SD (n = 3).

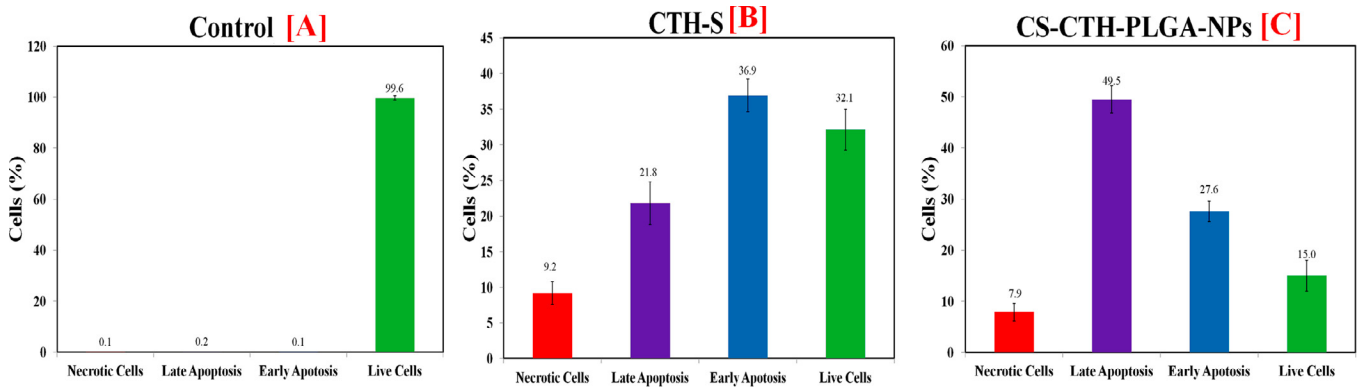

Fig. 7. Quantitative data for induction of apoptotic cell death by the (A) control group (untreated H1299 cells), (B) H1299 cells treated by CTH-solution and (C) CS-CTH-PLGA-NPs. Bar graph analysis showing higher total apoptotic cell death (early + late apoptosis) induced by CS-CTH-PLGA-NPs treatment compared to CTH-solution. Data are expressed as mean ± SD (n = 3). The data were analysed using one-way ANOVA followed by Turkey's post hoc test. The percentage of apoptotic cells in each group was compared with the control group; $p < 0.05$ indicates a significant difference.

of CAT-solution, CS-CTH-PLGA-NPs on cell death and proliferation. CAT-S and CS-CTH-PLGA-NPs has been given a concentration-dependent response at 24 h post-treatment which is and evidence through cell viability or toxicity against H1299 cells (Fig. 6B). CAT-S and CS-CTH-PLGA-NPs in difference at lesser concentrations have effects on cell death was insignificant but 50.0–100.0 $\mu g ml^{-1}$ higher concentrations have clear difference (Fig. 6B) followed by cytotoxic effects or cell death CS-CTH-PLGA-NPs being additionally marked and significant ($p \leq 0.050$) as compared to CAT-S (Fig. 6B). These results recommended an excellent cytotoxic potential of CAT in the form of CS-CTH-PLGA-NPs. Additionally, CS-CTH-PLGA-NPs showed smaller IC_{50} value i.e. 65.01 μg/mL as compared to CAT-S i.e. 97.14 μg/mL. Here, the results also suggested a higher cytotoxic effect of the CS-CTH-PLGA-NPs as compared to CAT-S. There was no toxicity with CS-PLGA-NPs (Placebo) at any time point or concentration (Fig. 6B). The cancerous cells (H1299) contained maximum anabolic demands respire mainly through glycolytic i.e. a maximum glucose or nutrient intake, production of lactate, and maximum rate of proliferation as compared to without-cancerous cells. It creates them higher exposure towards CAT-S or CS-CTH-PLGA-NPs. CAT-S or CS-CTH-PLGA-NPs exhibited maximum toxicity to cancer cells (H1299). It can be due to create the obstruction in the uptake of nutrition or membrane transporters inhibition for these cells i.e. usually absent in the non-cancerous cells. CS-CTH-PLGA-NPs have given results a maximum cytotoxic effect as compared to pure-CAT against H1299 cancerous cells. It can be accredited due to lower particle-size and fast uptake of CS-CTH-PLGA-NPs that make easy way to transport via different mechanisms for example passive transport/endocytosis into the cell by lipid bilayer as compared to the healthy cells. On the other hand, a different feature requires an inclusive evaluation at the molecular level to determine the accurate targets of these anti-cancerous preparations. IC_{50} is the main evaluation end point to determine the concentrations of drug. It means CAT loaded with nanoformulation i.e. CS-CTH-PLGA-NPs showed a greater cytotoxic potential than pure-CAT on the non-small cell lung cancer cells H1299.

3.6. CAT and CS-CTH-PLGA-NPs effects on cellular apoptosis

We determined the effects of CAT and their CS-CTH-PLGA-NPs nanoformulation mechanism by the estimation of treatment of cell apoptosis post-CAT through flow cytometry via an annexin V/FITC kit. A significantly induced was observed by cellular apoptosis of CAT (96.68 $\mu g ml^{-1}$ per 24.0 h) as compared to the without treated with CTH i.e. control group. CS-CTH-PLGA-NPs (65.01 $\mu g ml^{-1}$ per 24.0 h) was treated to H1299 cells, it was showed a high degree of apoptosis i.e. highly significant ($p < 0.050$) as compared to control as well as CAT-S. On the other side, we can see it CAT-S & CS-CTH-PLGA-NPs enhanced necrotic cells number when it compared to control group. Even if later on; the necrotic cells (%) was shown a little reduce than earlier (Fig. 7). Additionally, we have also observed CS-CTH-PLGA-NPs (76.7%)-treated group significantly higher ($p < 0.05$) than CAT-S (51.9%) based on results of early and late apoptotic cells. It has been suggested a strong apoptosis was induced with CS-CTH-PLGA-NPs (Fig. 7).

We evaluated prepared nano-formulation of catechin hydrate to assess whether this nano-formulation enhances its anti-tumor potential using NSCLC cell line H1299. To this end we found that CS-CTH-PLGA-NPs treated cells not only proved more cytotoxic (compared to CAT-alone) to the cancerous cells but also induced apoptosis in NSCLC cell line H1299. The effect was evident by increased percentage % of apoptotic cells in CS-CTH-PLGA-NPs group compared to both CAT-only and control treated cells.

3.7. Bioanalysis by UHPLC/MS/MS

CTH and IS MS and MS/MS scans were shown Fig. 8 and Fig. 9. All various matrixes chromatograms showed in Fig. 10 in which **[A & B]**, Extracted plasma and lungs homogenate (LH) without the CTH & with CTH **[C & D]**, extracted plasma & LH of CTH followed by **[E & F]** extracted plasma & LH of Quercetin. Mean recovery of CTH from LH and plasma (n = 6) was showed >79.68%. All observed matrixes of CTH exhibited a very good linearity (1.0 to 1000.0 ng ml^{-1}) i.e. $r^2 > 0.997$. 0.871 & 1.0 ng ml^{-1} was found the LOD and LOQ. The selectivity of all optimized-chromatograms for various matrixes of CTH has been proved. %CV (2.14–3.33% and 2.23–3.17%) was found whereas % accuracy (92.01–99.31% and 93.25–99.31%) exhibited for LH and PL of all QCs in Table 2. Various stability of storage parameters (long-term, bench-top, freeze thaw, and post-processing) for all types of quality control samples were presented in Table 3 (US–FDA, 2001; Ahmad et al., 2018b; Faiyazuddin et al., 2012).

3.8. Pulmonokinetics evaluation

The study reports for the first time, in-depth and detailed PKs for CS-CTH-PLGA-NPs where the NPs were administered via the major routes of oral, i.v. and intranasal in order to follow the

in vivo fate for developed NPs. The deposition of NPs in lungs and its engulfment is presented in Fig. 11 and Table 4. A C_{max} (maximum concentration of drug) for NPs in lungs was observed at 2.00 h [668.24 ± 29.66 ng/g] (i.n.; $p < 0.001$) >at 2.00 h [469.31 ± 32.96 ng/g] (i.v.; $p < 0.01$) >at 2.00 h [208.76 ± 17.01 ng/g] (oral). Lungs concentration of CAT was highest by intranasal route for CS-CTH-PLGA-NPs (Fig. 11, Table 4). Similarly, CS-CTH-PLGA-NPs have been showed enhanced the bioavailability as compared to CTH–S with the help of statistical evaluation for i.n. delivery of CAT. This is a very apparent observation via nose to lungs targeted potential (Monteillier et al., 2018; Dao et al., 2018; Worth et al., 2000; Jin et al., 2019).

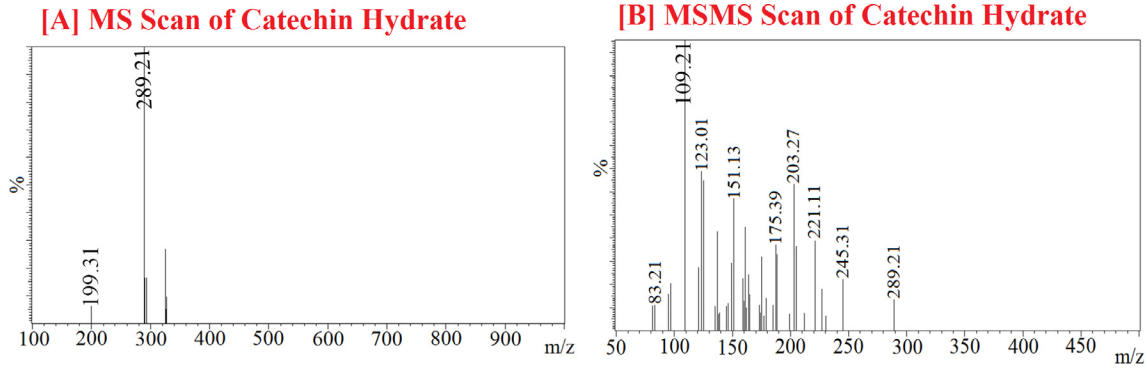

Fig. 8. Mass spectrum of (A) Catechin Hydrate (CTH) parent ion (protonated precursor $[M-H]^-$ ions at *m/z* 289.21) and (B) Catechin Hydrate (CTH) product ion (major fragmented product ion at *m/z* 109.21) showing fragmentation transitions.

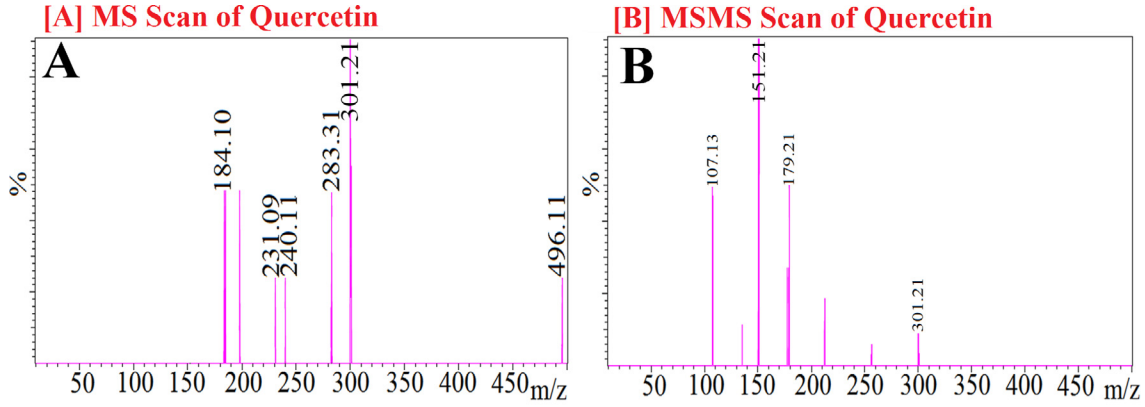

Fig. 9. Mass spectrum of, (A) Quercetin (IS) precursor ion (protonated precursor $[M-H]^-$ ions at *m/z* 301.21 and (B) IS product ion (major fragmented product ions at *m/z* 151.21) showing fragmentation transitions.

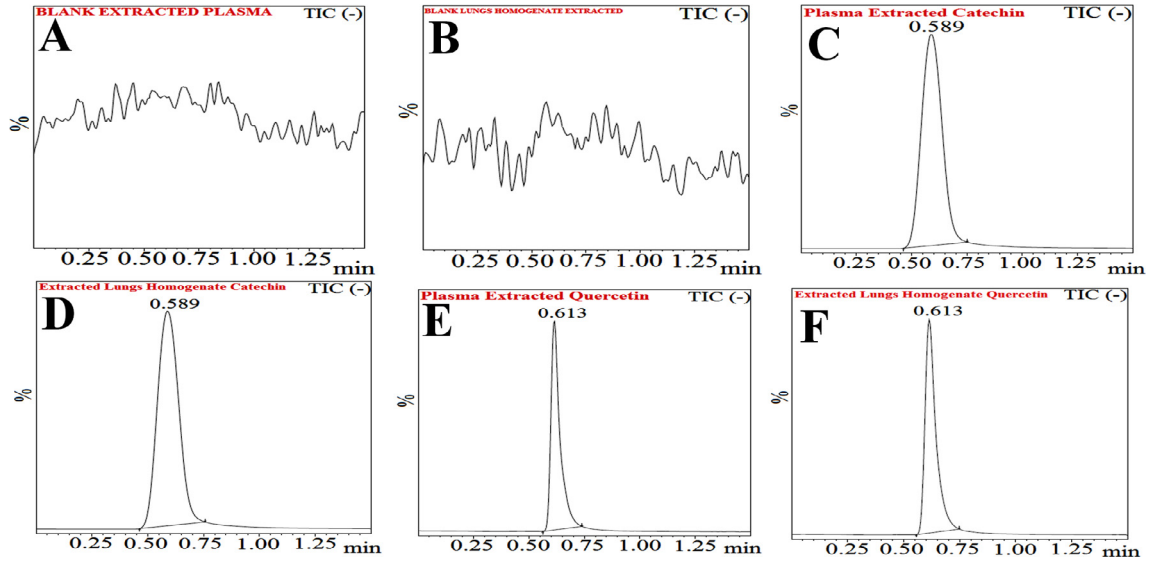

Fig. 10. Typical chromatograms of Extracted blank plasma **[A]**, Extracted blank lungs homogenate **[B]**, Plasma extracted Catechin Hydrate (CH) **[C]**, Extracted lungs homogenate Catechin Hydrate (CH) **[D]**, Plasma Extracted Quercetin (IS) **[E]**, and Extracted lungs homogenate Quercetin (IS) **[F]**.

Table 2
Validation: Precision and Accuracy Data for Catechin Hydrate in Lungs Homogenate and Plasma.

Biomatrix	Quality Controls Samples	Theoretical Concentration (ng mL^{-1}) or (ng g^{-1})	Intra-batch precision			Inter-batch precision			Recovery[c] (%)
			Observed Concentration (ng mL^{-1}) or (ng g^{-1}) ± S.D.	Accuracy[a] (%)	Precision[b] (%C.V.)	Observed Concentration (ng mL^{-1}) or (ng g^{-1}) ± S.D.	Accuracy[a] (%)	Precision[b] (%C.V.)	
Lungs Homogenate	LOQQC	1.01	0.98 ± 0.021	97.03	2.14	0.96 ± 0.025	95.05	2.60	80.01
	LQC	2.91	2.89 ± 0.096	99.31	3.32	2.88 ± 0.096	98.97	3.33	79.68
	MQC	420.0	392.11 ± 9.60	93.36	2.45	386.45 ± 8.86	92.01	2.29	82.61
	HQC	805.0	795.64 ± 18.74	98.84	2.36	783.64 ± 17.64	97.35	2.25	79.94
Plasma	LOQQC	1.01	0.97 ± 0.028	96.04	2.89	0.96 ± 0.028	95.05	2.92	80.36
	LQC	2.91	2.89 ± 0.086	99.31	2.98	2.87 ± 0.091	98.63	3.17	79.94
	MQC	420.0	394.54 ± 10.01	93.94	2.54	391.64 ± 9.94	93.25	2.54	83.02
	HQC	805.0	792.16 ± 17.64	98.40	2.23	785.38 ± 18.66	97.56	2.38	80.39

Values (Mean ± SD) are derived from 6 replicates: [a]Accuracy (%) = Mean value of [(mean observed concentration)/(theoretical concentration)] × 100; [b]Precision (%): Coefficient of variance (percentage) = standard deviation divided by mean concentration found × 100; [c]Recovery (%) = Mean value of (peak height (mV) obtained from extracted biological sample)/(peak height (mV) obtained from aqueous sample) × 100.

Table 3
Validation: Stability Data for Catechin Hydrate in Lungs Homogenate and Plasma.

Exposure condition	LQC (2.91 ng/mL or ng g^{-1})		MQC(420.00 ng/mL or ng g^{-1})		HQC (805.00 ng/mL or ng g^{-1})	
	Lungs Homogenate	Plasma	Lungs Homogenate	Plasma	Lungs Homogenate	Plasma
Long term stability; recovery (ng) after storage (−80.0 °C)						
Previous day	2.88 ± 0.07	2.86 ± 0.03	405.24 ± 11.02	406.57 ± 10.32	799.36 ± 19.21	800.34 ± 18.61
30th Day	2.81 ± 0.06 (97.57%)	2.79 ± 0.04 (97.55%)	379.91 ± 910.31 (93.75%)	381.61 ± 9.61 (93.86%)	788.21 ± 18.22 (98.61%)	787.54 ± 17.36 (98.40%)
Freeze–thaw stress; recovery (ng) after freeze–thaw cycles (−80.0 °C to 25.0 °C)						
Pre-Cycle	2.89 ± 0.05	2.90 ± 0.03	406.01 ± 9.33	406.34 ± 8.55	801.15 ± 21.61	800.31 ± 20.36
First Cycle	2.78 ± 0.06 (96.19%)	2.80 ± 0.04 (96.55%)	391.31 ± 9.22 (96.38%)	389.06 ± 9.06 (95.75%)	791.31 ± 20.14 (98.77%)	789.21 ± 19.47 (98.61%)
Second Cycle	2.70 ± 0.05 (93.43%)	2.71 ± 0.03 (93.45%)	379.64 ± 8.17 (93.51)	371.69 ± 8.11 (91.47%)	779.64 ± 19.61 (97.32%)	778.95 ± 20.14 (97.33%)
Third Cycle	2.61 ± 0.06 (90.31%)	2.59 ± 0.05 (89.31%)	361.24 ± 8.07 (88.97%)	366.17 ± 9.03 (90.11%)	770.06 ± 20.14 (96.12%)	771.28 ± 21.34 (96.37%)
Bench top stability; recovery (ng) at room temperature (25.0 °C)						
0 hr	2.88 ± 0.04	2.85 ± 0.03	407.13 ± 8.61	404.34 ± 9.06	799.97 ± 21.14	801.21 ± 21.67
24 hr	2.72 ± 0.04 (94.44%)	2.73 ± 0.04 (95.79%)	384.61 ± 9.18 (94.47%)	389.43 ± 9.63 (96.31%)	788.24 ± 19.61 (98.53%)	783.64 ± 20.34 (97.81%)
Post processing stability; recovery (ng) after storage in auto sampler (4.0 °C)						
0 hr	2.89 ± 0.05	2.87 ± 0.03	405.18 ± 8.34	406.11 ± 10.24	800.11 ± 20.36	798.24 ± 22.06
4 hr	2.79 ± 0.04 (96.54%)	2.75 ± 0.06 (95.82%)	381.64 ± 8.21 (94.19%)	391.34 ± 9.61 (96.36%)	790.32 ± 19.64 (98.78%)	788.36 ± 21.34 (98.76%)

Values (Mean ± SD) are derived from six replicates. Figures in parenthesis represent analyte concentration (%) relative to time zero. Theoretical contents; LQC: 2.91 ng mL^{-1}; MQC: 420.0 ng mL^{-1}; and HQC: 805.0 ng mL^{-1}.

3.9. In vivo Histopathological examination of CS-CTH-PLGA-NPs toxicity

The histological micrographs of lung specimens collected from rat's post seven-days of exposure to 0.90% saline and treated with CS-CTH-PLGA-NPs by intranasal are depicted in Fig. 12. There was no apparent histopathologic alteration in the lungs tissues (Fig. 12B) as compared to Normal Saline treated (control group, Fig. 12A). CS-CTH-PLGA-NPs did not cause any toxicity. These results indicate that CS-CTH-PLGA-NPs are safe and exhibited no obvious toxic effects on the rat's lungs. Exposure of above mentioned particles at mentioned dose does not produce any mortality and also and no abnormal findings in the treated rats with CS-CTH-PLGA-NPs were observed (Menon et al., 2017; Gelli et al., 2015; Ahmad et al., 2020d).

4. Conclusion

A solvent evaporation (double emulsion) was used to formulate CS-CTH-PLGA-NPs and their optimization was evaluated by low PDI, smaller size of particles, greater EE with high DL and spherical

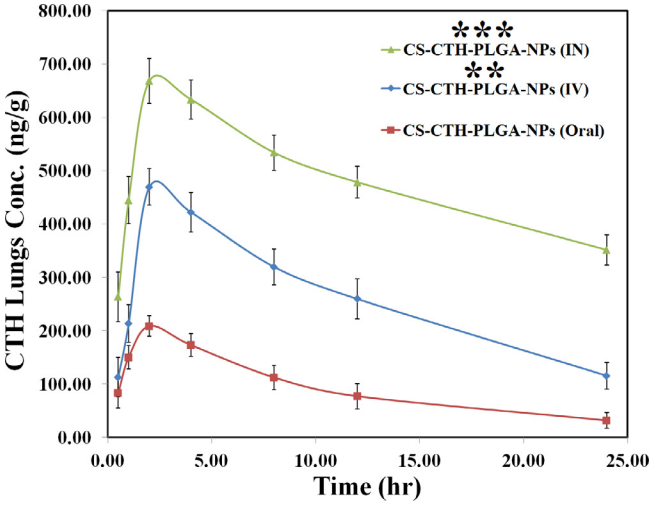

Fig. 11. Pulmonary Pharmacokinetic Parameters Study of Catechin Hydrate in wistar rats after 10 mg/kg single dose of CS–CTH–PLGA–NPs (intravenous), CS–CTH–PLGA–NPs (Oral), and CS–CTH–PLGA–NPs (Intranasal). Significantly high AUC was achieved with CS–BUD–PLGA–NPs (Intranasal) ($p < 0.001$, mean ± SD, n = 6).

Table 4
Pulmonary Pharmacokinetic parameters of catechin hydrate after single dose (10 mg/kg body weight) of CS-coated-CTH-loaded-PLGA-NPs given by different routes (mean ± SD n = 6).

Parameters	CS- CTH-PLGA-NPs (IV)	CS- CTH-PLGA-NPs (Oral)	CS- CTH-PLGA-NPs (Intranasal)
Cmax (ng/ml or ng/g)	469.31 ± 32.96**	208.76 ± 17.01	668.24 ± 29.66***
Tmax (h)	2.00	2.00	2.00
$AUC_{0\text{-}t}$ (min ng/ml) or min ng/g)	6208.00 ± 89.67**	2223.77 ± 42.08	11370.02 ± 191.05***
$t_{1/2}$ (h)	26.47	10.82	91.16
K_e (h^{-1})	0.02619	0.06408	0.00760
$AUC_{0\text{-}\infty}$ (min ng/ml) or min ng/g)	10628.91 ± 153.0.78**	2720.50 ± 83.91	57567.74 ± 212.15***

AUC_{0-t}, Area under the lungs concentration to time curve; $AUC_{0-\infty}$, Area under the plasma concentration to infinite time curve; Cmax, maximum lungs concentration at time t; $t_{1/2}$, mean elimination half-life; and Ke, Elimination Rate Constant. Data are represented as mean ± SD (n = 3). Significantly high AUC and Cmax were achieved with CS–CTH–PLGA–NPs (Intranasal) ***($p < 0.001$), followed by CS-CTH-PLGA-NPs (IV) **($p < 0.01$) mean ± SD, n = 6).

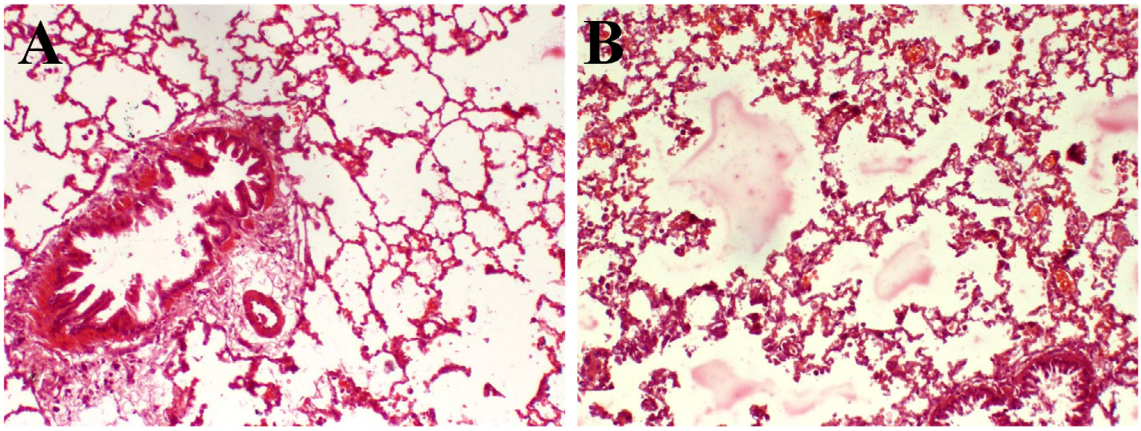

Fig. 12. *In Vivo* Safety of CS–coated–CTH–loaded–PLGA–NPs: Histopathological evaluation of rat tissues: Normal Saline **(A),** and treated with CS–CTH–PLGA–NPs **(B)** seven days after exposure. The photomicrographs do not shown any evidence of toxicity from the CS-CTH-PLGA-NPs and were no apparent histopathologic changes in the lungs tissues (Fig. 12B) as compared to Normal Saline treated (control group, Fig. 12A) (n = 3, Scale = 100 μm).

shape. CAT-release was optimized successfully based on a sustained and control release form followed by successfully delivered to lungs with extended retention from nose-to-lungs with passed up hepatic first pass metabolism and also greater nasal permeation upto 24-h for lungs cancer targeting. A +ve zeta potential of the CS coated NPs support binding of the nanocarrier to the cancer cells to exert enhanced cytotoxic potential of the formulation with superior apoptotic potential and cell cycle arrest when compared with CAT alone, CS-CTH-PLGA-NPs exhibited greater apoptotic cell death and cytotoxic in the H1299 cell line. A UPLC-MS/MS method was optimized and validated successfully for the application on pulmokinetics studies of optimized-CS-CTH-PLGA-NPs. At the end, safety of the optimized nanoparticles has been established on the basis of the above results at the time of lungs toxicity studies. At last in this study, CS-CTH-PLGA-NPs have been successfully developed and it can be effectively use as a novel, non-invasive, safe, and effective treatment for lungs targeting in the treatment of lung cancer.

Funding

The authors were not received any funds.

Declaration of Competing Interest

There is no competing interest's in-between the authors.

Acknowledgments

The authors are very grateful thanks to Animal House, IRMC, Imam Abdulrahman Bin Faisal University, Saudi Arabia.

References

Ahmad, N., Ahmad, R., Ahmad, F.J., Ahmad, W., Alam, M.A., Amir, M., Ali, A., 2020a. Poloxamer-chitosan-based Naringenin nanoformulation used in brain targeting for the treatment of cerebral ischemia. Saudi J. Biol. Sci. 27 (1), 500–517. https://doi.org/10.1016/j.sjbs.2019.11.008.

Ahmad, N., Ahmad, R., Alam, M.A., Ahmad, F.J., 2018a. Enhancement of oral bioavailability of doxorubicin through surface modified biodegradable polymeric nanoparticles. Chem. Cent. J. 12 (1), 65. https://doi.org/10.1186/s13065-018-0434-1.

Ahmad, N., Ahmad, R., Alam, M.A., Samim, M., Iqbal, Z., Ahmad, F.J., 2016a. Quantification and evaluation of thymoquinone loaded mucoadhesive nanoemulsion for treatment of cerebral ischemia. Int. J. Biol. Macromol. 88, 320–332. https://doi.org/10.1016/j.ijbiomac.2016.03.019.

Ahmad, N., Ahmad, R., Naqvi, A.A., Alam, M.A., Samim, M., Iqbal, Z., Ahmad, F.J., 2016b. Quantification of rutin in rat's brain by UHPLC/ESI-Q-TOF-MS/MS after intranasal administration of rutin loaded chitosan nanoparticles. EXCLI J. 15, 518–531. https://doi.org/10.17179/excli2016-361.

Ahmad, N., Alam, M.A., Ahmad, R., Umar, S., Ahmad, F.J., 2018b. Improvement of oral efficacy of Irinotecan through biodegradable polymeric nanoparticles through in vitro and in vivo investigations. J. Microencapsul. 35 (4), 327–343. https://doi.org/10.1080/02652048.2018.1485755.

Ahmad, N., Al-Subaiec, A.M., Ahmad, R., Sharma, S., Alam, M.A., Ashafaq, M., Rub, R. A., Ahmad, F.J., 2019. Brain-targeted glycyrrhizic-acid-loaded surface decorated nanoparticles for treatment of cerebral ischaemia and its toxicity assessment. Artif. Cells Nanomed. Biotechnol. 47 (1), 475–490. https://doi.org/10.1080/21691401.2018.1561458.

Ahmad, N., Ahmad, R., Alrasheed, R.A., Almatar, H.M.A., Al-Ramadan, A.S., Amir, M., Sarafroz, M., 2020b. Quantification and evaluations of catechin hydrate polymeric nanoparticles used in brain targeting for the treatment of epilepsy. Pharmaceutics 12 (3), E203. https://doi.org/10.3390/pharmaceutics12030203.

Ahmad, N., 2017. Rasagiline-encapsulated chitosan-coated PLGA nanoparticles targeted to the brain in the treatment of parkinson's disease. J. Liq. Chromatogr. Relat. Technol. 40 (13), 677–690. https://doi.org/10.1080/10826076.2017.1343735.

Ahmad, N., Ahmad, R., Al Qatifi, S., Alessa, M., Al Hajji, H., Sarafroz, M., 2020c. A bioanalytical UHPLC based method used for the quantification of Thymoquinone-loaded-PLGA-nanoparticles in the treatment of epilepsy. BMC Chem. 14 (1), 10. https://doi.org/10.1186/s13065-020-0664-x.

Ahmad, N., Ahmad, R., Almakhamel, M.Z., Ansari, K., Amir, M., Ahmad, W., Ali, A., Ahmad, F.J., 2020d. A comparative pulmonary pharmacokinetic study of

budesonide using polymeric nanoparticles targeted to the lungs in treatment of asthma. Artif. Cells Nanomed. Biotechnol. 48 (1), 749–762. https://doi.org/10.1080/21691401.2020.1748640.
Akowuah, G., Mariam, A., Chin, J., 2009. The effect of extraction temperature on total phenols and antioxidant activity of *Gynura procumbens* leaf. Pharmacogn. Mag. 5 (17), 81–85.
Alshatwi, A.A., Athinarayanan, J., Subbarayan, P.V., 2015. Green synthesis of platinum nanoparticles that induce cell death and G2/M-phase cell cycle arrest in human cervical cancer cells. J. Mater. Sci. Mater. Med. 26 (1), 5330. https://doi.org/10.1007/s10856-014-5330-1.
Alshatwi, A.A., 2010. Catechin hydrate suppresses MCF-7 proliferation through TP53/Caspase-mediated apoptosis. J. Exp. Clin. Cancer Res. 29 (1), 167. https://doi.org/10.1186/1756-9966-29-167.
Bahuguna, A., Khan, I., Bajpai, V.K., Kang, S.C., 2017. MTT assay to evaluate the cytotoxic potential of a drug. Bangladesh J. Pharmacol. 12 (2), 115–118. https://doi.org/10.3329/bjp.v12i2.30892.
Baliga, M.S., Meleth, S., Katiyar, S.K., 2005. Growth inhibitory and antimetastatic effect of green tea polyphenols on metastasis-specific mouse mammary carcinoma 4T1 cells *in vitro* and *in vivo* systems. Clin. Cancer Res. 11, 1918–1927. https://doi.org/10.1158/1078-0432.CCR-04-1976.
Bao, W., Liu, R., Wang, Y., Wang, F., Xia, G., Zhang, H., Li, X., Yin, H., Chen, B., 2015. PLGA-PLL-PEG-Tf-based targeted nanoparticles drug delivery system enhance antitumor efficacy via intrinsic apoptosis pathway. Int. J. Nanomedicine. 10, 557–566. https://doi.org/10.2147/IJN.S75090.
Brown, J.S., Eraut, D., Trask, C., Davison, A.G., 1996. Age and the treatment of lung cancer. Thorax 51 (6), 564–568. https://doi.org/10.1136/thx.51.6.564.
Budhian, A., Siegel, S.J., Winey, K.I., 2008. Controlling the in vitro release profiles for a system of haloperidol-loaded PLGA nanoparticles. Int. J. Pharm. 346 (1–2), 151–159. https://doi.org/10.1016/j.ijpharm.2007.06.011.
Chang, C.L., Wub, R.T., 2011. Quantification of (+)-catechin and (−)-epicatechin in coconut water by LC–MS. Food Chem. 126, 710–717.
Choudhury, H., Gorain, B., Pandey, M., Khurana, R.K., Kesharwani, P., 2019. Strategizing biodegradable polymeric nanoparticles to cross the biological barriers for cancer targeting. Int. J. Pharm. 565, 509–522. https://doi.org/10.1016/j.ijpharm.2019.05.042.
Dao, D.T., Vuong, J.T., Anez-Bustillos, L., Pan, A., Mitchell, P.D., Fell, G.L., Baker, M.A., Bielenberg, D.R., Puder, M., 2018. Intranasal delivery of VEGF enhances compensatory lung growth in mice. PLoS One. 13, (6). https://doi.org/10.1371/journal.pone.0198700 e0198700.
Dias, A.L., Rozet, E., Larondelle, Y., Hubert, P., Rogez, H., Quetin-Leclercq, J., 2013. Development and validation of an UHPLC–LTQ-Orbitrap MS method for non-anthocyanin flavonoids quantification in Euterpe oleracea juice. Anal. Bioanal. Chem. 405, 9235–9249. https://doi.org/10.1007/s00216-013-7325-z.
Dube, A., Nicolazzo, J.A., Larson, I., 2010. Chitosan nanoparticles enhance the intestinal absorption of the green tea catechins (+)-catechin and (-)-epigallocatechin gallate. Eur. J. Pharm. Sci. 41 (2), 219–225. https://doi.org/10.1016/j.ejps.2010.06.010.
Faiyazuddin, M., Ahmad, N., Khar, R.K., Bhatnagar, A., Ahmad, F.J., 2012. Stabilized terbutaline submicron drug aerosol for deep lungs deposition: drug assay, pulmonokinetics and biodistribution by UHPLC/ESI-q-TOF-MS method. Int. J. Pharm. 434 (1–2), 59–69. https://doi.org/10.1016/j.ijpharm.2012.05.007.
Fernandez-Urrusuno, R., Romani, D., Calvo, D., 1999. Development of a freeze dried formulation of insulin-loaded chitosan nanoparticles intended for nasal administration. STP Pharm. Sci. 9, 429–436.
Gelli, K., Porika, M., Anreddy, R.N., 2015. Assessment of pulmonary toxicity of MgO nanoparticles in rats. Environ. Toxicol. 30 (3), 308–314. https://doi.org/10.1002/tox.21908.
Glade, M.J., 1997. Food, nutrition, and the prevention of cancer: 1999. A global perspective. American Institute for Cancer Research/World Cancer Research Fund. American Institute for Cancer Research. Nutrition 15 (6), 523–526. https://doi.org/10.1016/S0899-9007(99)00021-0.
Gorain, B., Choudhury, H., Pandey, M., Kesharwani, P., 2018. Paclitaxel loaded vitamin E-TPGS nanoparticles for cancer therapy. Mater. Sci. Eng. C Mater. Biol. Appl. 91, 868–880. https://doi.org/10.1016/j.msec.2018.05.054.
Green, P.M., Guerrier-Adams, S., Okunji, P.O., Schiavone, D., Smith, J.E., 2013. African American health disparities in lung cancer. Clin. J. Oncol. Nurs. 17 (2), 180–186. https://doi.org/10.1188/13.CJON.180-186.
Gujar, J.G., Chattopadhyay, S., Wagh, S.J., Gaikar, V.G., 2010. Experimental and modeling studies on extraction of catechin hydrate and epicatechin from Indian green tea leaves. Can. J. Chem. Eng. 88 (2), 232–240. https://doi.org/10.1002/cjce.20271.
Ian, R.R., Dreosti, I.E., 1998. Protection by black tea and green tea against UVB and UVA+B induced skin cancer in hairless mice. Mutat. Res. 422 (1), 191–199. https://doi.org/10.1016/S0027-5107(98)00192-4.
Jaitz, L., Siegl, K., Eder, R., Rak, G., Abranko, L., Koellensperger, G., Hann, S., 2010. LC–MS/MS analysis of phenols for classification of red wine according to geographic origin, grape variety and vintage. Food Chem. 122, 366–372. https://doi.org/10.1016/j.foodchem.2010.02.053.
Jeong, H., Phan, A.N.H., Choi, J.W., 2017. Anti-cancer effects of polyphenolic compounds in epidermal growth factor receptor tyrosine kinase inhibitor-resistant non-small cell lung cancer. Pharmacogn. Mag. 13 (52), 595–599. https://doi.org/10.4103/pm.pm_535_16.
Jin, R., Hu, S., Liu, X., Guan, R., Lu, L., Lin, R., 2019. Intranasal instillation of miR-410 targeting IL-4/IL-13 attenuates airway inflammation in OVA-induced asthmatic mice. Mol. Med. Rep. 19 (2), 895–900. https://doi.org/10.3892/mmr.2018.9703.
Justus, C.R., Dong, L., Yang, L.V., 2013. Acidic tumor microenvironment and pH-sensing G protein-coupled receptors. Front. Physiol. 4, 354. https://doi.org/10.3389/fphys.2013.00354.
Kang, W.S., Lim, I.H., Yuk, D.Y., Chung, K.H., Park, J.B., Yoo, H.S., Yun, Y.P., 1999. Antithrombotic activities of green tea catechins and (−)-epigallocatechin gallate thromb. Res. 96 (3), 229–237. https://doi.org/10.1016/s0049-3848(99)00104-8.
Krishnaswamy, K., Vali, H., Orsat, V., 2014. Value-adding to grape waste: green synthesis of gold nanoparticles. J. Food Sci. 142, 210–220. https://doi.org/10.1016/j.jfoodeng.2014.06.014.
Lai, H.Y., Lim, Y.Y., Kim, K.H., 2017. Isolation and characterisation of a proanthocyanidin with antioxidative, antibacterial and anti-cancer properties from fern *Blechnum orientale*. Pharmacogn. Mag. 13 (49), 31–37. https://doi.org/10.4103/0973-1296.197659.
Lendoiro, E., de Castro, A., Fernández-Vega, H., Cela-Pérez, M.C., López-Vilariño, J.M., González-Rodríguez, M.V., Cruz, A., López-Rivadulla, M., 2014. Molecularly imprinted polymer for selective determination of Δ9-tetrahydrocannabinol and 11-nor-Δ9-tetrahydrocannabinol carboxylic acid using LC–MS/MS in urine and oral fluid. Anal. Bioanal. Chem. 406 (15), 3589–3597. https://doi.org/10.1007/s00216-013-7599-1.
Masami, S., Sachiko, O., Naoko, S., Eisaburo, S., Satoru, M., Kazue, I., Kei, N., Hirota, F., 1999. Green tea and cancer chemoprevention. Mutat. Res. 428 (1–2), 339–344. https://doi.org/10.1016/S1383-5742(99)00059-9.
Md, S., Khan, R.A., Mustafa, G., Chuttani, K., Baboota, S., Sahni, J.K., Ali, J., 2013. Bromocriptine loaded chitosan nanoparticles intended for direct nose to brain delivery: pharmacodynamic, pharmacokinetic and scintigraphy study in mice model. Eur. J. Pharm. Sci. 48 (3), 393–405. https://doi.org/10.1016/j.ejps.2012.12.007.
Menon, J.U., Kuriakose, A., Iyer, R., Hernandez, E., Gandee, L., Zhang, S., Takahashi, M., Zhang, Z., Saha, D., Nguyen, K.T., 2017. Dual-drug containing core-shell nanoparticles for lung cancer therapy. Sci. Rep. 7 (1), 13249. https://doi.org/10.1038/s41598-017-13320-4.
Merken, H.M., Beecher, G.R., 2000. Measurement of food flavonoids by high-performance liquid chromatography: a review. J. Agricult. Food Chem. 48 (3), 577–599. https://doi.org/10.1021/jf990872o.
Min, J., Shen, H., Xi, W., Wang, Q., Yin, L., Zhang, Y., Yu, Y., Yang, Q., Wang, Z.N., 2018. Synergistic anticancer activity of combined use of caffeic acid with paclitaxel enhances apoptosis of non-small-cell lung cancer H1299 Cells in vivo and in vitro. Cell Physiol. Biochem. 48 (4), 1433–1442. https://doi.org/10.1159/000492253.
Monteillier, A., Voisin, A., Furrer, P., Allémann, E., Cuendet, M., 2018. Intranasal administration of resveratrol successfully prevents lung cancer in A/J mice. Sci. Rep. 8 (1), 14257. https://doi.org/10.1038/s41598-018-32423-0.
Mukhtar, H., Ahmad, N., 2000. Tea polyphenols: prevention of cancer and optimizing health. Am. J. Clin. Nutr. 71 (6 Suppl). https://doi.org/10.1093/ajcn/71.6.1698S. 1698S-702S; discussion 1703S-4S.
Nafee, N., Taetz, S., Schneider, M., Schaefer, U.F., Lehr, C.M., 2007. Chitosan-coated PLGA nanoparticles for DNA/RNA delivery: effect of the formulation parameters on complexation and transfection of antisense oligonucleotides. Nanomedicine. 3 (3), 173–183. https://doi.org/10.1016/j.nano.2007.03.006.
Natarajan, C.P., Ramamani, S., Leelavathi, D.E., Shakunthala, R., Bhatia, D.S., Subrahmanyan, Y., 1962. Studies on the brewing of tea. Food Sci. 11, 321–332.
Nelson, B.C., Sharpless, K.E., 2003. Quantification of the predominant monomeric catechins in baking chocolate standard reference material by LC/APCI-MS. J. Agric. Food Chem. 51 (3), 531–537. https://doi.org/10.1021/jf0207474.
Pandey, K.B., Rizvi, S.I., 2009. Plant polyphenols as dietary antioxidants in human health and disease. Oxid. Med. Cell Longev. 2 (5), 270–278. https://doi.org/10.4161/oxim.2.5.9498.
Pandey, M., Choudhury, H., Yeun, O.C., Yin, H.M., Lynn, T.W., Tine, C.L.Y., Wi, N.S., Yen, K.C.C., Phing, C.S., Kesharwani, P., Bhattamisra, S.K., Gorain, B., 2018. Perspectives of nanoemulsion strategies in the improvement of oral, parenteral and transdermal chemotherapy. Curr. Pharm. Biotechnol. 19 (4), 276–292. https://doi.org/10.2174/1389201019666180605125234.
Parveen, S., Sahoo, S.K., 2011. Long circulating chitosan/PEG blended PLGA nanoparticle for tumor drug delivery. Eur. J. Pharmacol. 670 (2–3), 372–383. https://doi.org/10.1016/j.ejphar.2011.09.023.
Poon, G.K., 1998. Analysis of catechins in tea extracts by liquid chromatography–electrospray ionization mass spectrometry. J. Chromatogr. A. 794, 63–74.
Raparia, K., Villa, C., Decamp, M.M., Patel, J.D., Mehta, M.P., 2013. Molecular profiling in non-small cell lung cancer: a step toward personalized medicine. Arch. Pathol. Lab. Med. 137 (4), 481–491. https://doi.org/10.5858/arpa.2012-0287-RA.
Richter, T., Keipert, S., 2004. In vitro permeation studies comparing bovine nasal mucosa, porcine cornea and artificial membrane: androstenedione in microemulsions and their components. Eur. J. Pharm. Biopharm. 58 (1), 137–143. https://doi.org/10.1016/j.ejpb.2004.03.010.
Sahoo, S.K., Panyam, J., Prabha, S., Labhasetwar, V., 2002. Residual polyvinyl alcohol associated with poly (D, L-lactide-co-glycolide) nanoparticles affects their physical properties and cellular uptake. J. Control Release. 82 (1), 105–114. https://doi.org/10.1016/S0168-3659(02)00127-X.
Sapozhnikova, Y., 2014. Development of liquid chromatography-tandem mass spectrometry method for analysis of polyphenolic compounds in liquid samples of grape juice, green tea and coffee. Food Chem. 150, 87–93. https://doi.org/10.1016/j.foodchem.2013.10.131.
Shahid, A., Ali, R., Ali, N., Hasan, S.K., Bernwal, P., Afzal, S.M., Vafa, A., Sultana, S., 2016. Modulatory effects of catechin hydrate against genotoxicity, oxidative

stress, inflammation and apoptosis induced by benzo(a)pyrene in mice. Food Chem. Toxicol. 92, 64–74. https://doi.org/10.1016/j.fct.2016.03.021.
Siddiqi, K.S., Husen, A., 2016. Green synthesis, characterization and uses of palladium/platinum nanoparticles. Nanoscale Res. Lett. 11 (1), 482. https://doi.org/10.1186/s11671-016-1695-z.
Spiro, M., Jago, D.S., 1982. Kinetics and equilibria of tea infusion part III: rotating disc experiments interpreted by a steady-state model. J. Chem. Soc. Faraday Trans. 1 (78), 295–305. https://doi.org/10.1039/F19827800295.
Svoboda, P., Vlčková, H., Nováková, L., 2015. Development and validation of UHPLC–MS/MS method for determination of eight naturally occurring catechin derivatives in various tea samples and the role of matrix effects. J. Pharm. Biomed. Anal. 114, 62–70. https://doi.org/10.1016/j.jpba.2015.04.026.
Taamalli, A., Arráez-Román, D., Abaza, L., Iswaldi, I., Fernández-Gutiérrez, A., Zarrouk, M., Segura-Carretero, A., 2015. LC–MS-based metabolite profiling of methanolic extracts from the medicinal and aromatic species *Mentha pulegium* and *Origanum majorana*. Phytochem. Anal. 26 (5), 320–330. https://doi.org/10.1002/pca.2566.
Taparia, S., Khanna, A., 2016. Effect of procyanidin-rich extract from natural cocoa powder on cellular viability, cell cycle progression, and chemoresistance in human epithelial ovarian carcinoma cell lines. Pharmacogn. Mag. 12 (Suppl 2), S109–15. https://doi.org/10.4103/0973-1296.182164.
Tolosa, L., Donato, M.T., Gómez-Lechón, M.J., 2015. General cytotoxicity assessment by means of the MTT assay. Methods Mol. Biol. 1250, 333–348. https://doi.org/10.1007/978-1-4939-2074-7_26.
US FDA, 2001. Guidance for Industry Bioanalytical Method Validation; 2001. Available from: http://www.fda.gov/downloads/Drugs/GuidanceComplianceRegulatoryInformation/Guidances/UCM070107.pdf. [Last accessed on 2018 May 24].
Wang, H., Helliwell, K., 2000. Epimerisation of catechins in green tea infusions. Food Chem. 70 (3), 337–344. https://doi.org/10.1016/S0308-8146(00)00099-6.
Wang, Y., Li, P., Kong, L., 2013. Chitosan-modified PLGA nanoparticles with versatile surface for improved drug delivery. Aaps Pharmscitech. 14 (2), 585–592. https://doi.org/10.1208/s12249-013-9943-3.
Worth, L.L., Jia, S.F., Zhou, Z., Chen, L., Kleinerman, E.S., 2000. Intranasal therapy with an adenoviral vector containing the murine interleukin-12 gene eradicates osteosarcoma lung metastases. Clin. Cancer Res. 6 (9), 3713–3718.